Journal of Membrane Science 574 (2019) 100–111

Contents lists available at ScienceDirect

Journal of Membrane Science

journal homepage: www.elsevier.com/locate/memsci

Gas and water vapor sorption and diffusion in a triptycene-based polybenzoxazole: effect of temperature and pressure and predicting of mixed gas sorption

Valerio Loianno[a,b], Shuangjiang Luo[c], Qinnan Zhang[c], Ruilan Guo[c], Michele Galizia[a,*]

[a] School of Chemical, Biological and Materials Engineering, University of Oklahoma, 100 E. Boyd Street, Norman 73019, OK, USA
[b] Department of Chemical, Materials and Industrial Production Engineering, University of Naples Federico II, p.le Tecchio 80, 80125 Naples, Italy
[c] Department of Chemical and Biomolecular Engineering, University of Notre Dame, 205 McCourtney Hall, Notre Dame 46556, IN, USA

ARTICLE INFO

Keywords:
Gas separation
Iptycene-based polymers
Sorption
Competitive sorption

ABSTRACT

Fundamental gas transport properties of a novel thermally rearranged polymer (TPBO) prepared from a co-polyimide precursor with controlled triptycene molar content are discussed. He, N_2, CH_4, CO_2 and C_2H_6 sorption isotherms were experimentally measured in the range 5–50 °C and up to 32 atm and analyzed with the dual mode model. Water vapor sorption and diffusion at 35 °C was also investigated. TPBO exhibits larger gas and vapor sorption capacity relative to previously reported thermally rearranged polymers. The dual mode parameters retrieved from the analysis of single gas sorption isotherms were used to estimate *a priori* the sorption behavior in mixed gas conditions. The predicted mixed gas solubility-selectivity is significantly higher than ideal solubility-selectivity and it is comparable to that exhibited by other glassy polymers. Gas and vapor diffusion coefficients in TPBO were estimated from the solution-diffusion model and from sorption kinetics, respectively, and are larger than in previously reported thermally rearranged polymers. The dual sorption-mobility model indicates that the polymer rigidity significantly affects gas diffusion coefficients. CO_2/CH_4 diffusivity-selectivity was larger than in other glassy polymers, pointing out the superior size-sieving ability provided by triptycene units. Water vapor sorption experiments revealed that TPBO is more hydrophilic relative to previously reported thermally rearranged polymers: theoretical models were exploited to speculate water vapor distribution in the polymer matrix.

1. Introduction

Membrane gas separation is raising attention in chemical, petrochemical and pharmaceutical industry. Despite current sales in the membrane market are in the range of $1.5 billion/year, the route towards large scale use of membrane separations is not yet completed [1]. The lack of membrane materials endowed with adequate performance is the real roadblock to progress in this area [1]. Materials exhibiting high permeability and selectivity, combined with mechanical robustness, are sought to make membrane separations competitive with traditional thermal processes, such as distillation or absorption [1]. Unfortunately, a trade-off exists between membrane permeability (i.e., productivity) and selectivity (i.e., separation efficiency) [2,3]. Ever since Robeson first pointed out the existence of this trade-off, significant efforts have been made to modify or synthesize materials with superior performance [1]. In recent years, thermally rearranged (TR) polymers [4], as well as polymers of intrinsic microporosity (PIMs) [5,6] raised special attention as they surpass the upper bound in several industrially-relevant applications.

Besides having good transport and mechanical properties, ideal membrane materials should maintain their properties stable over time and exhibit acceptable resistance to plasticization in applications were CO_2 or condensable vapors are involved. Unfortunately, materials that meet all these requirements are rare. The issue of physical aging, that is, the loss of free volume over time, is especially crucial. Physical aging is related to the non-equilibrium nature of glassy polymers, which tend to relax the excess free volume frozen in their structure to approach “true” equilibrium conditions. The conformational, non-equilibrium free volume available for gas transport in glassy polymers is intrinsically unstable, which makes transport properties unstable as well [7,8]. Due to the large amount of excess conformational free volume frozen in their structure, PIMs significantly depart from equilibrium conditions, which makes them subject to physical aging [9].

Incorporating triptycene structures into high performance polymers

* Corresponding author.
E-mail address: mgalizia@ou.edu (M. Galizia).

https://doi.org/10.1016/j.memsci.2018.12.054
Received 10 November 2018; Received in revised form 17 December 2018; Accepted 19 December 2018
Available online 21 December 2018

is a viable route to prepare materials with superior and stable separation performance [7,10–17]. Indeed, due to their microporous nature, the internal free volume provided by triptycene units is not related to the non-equilibrium conformation, but to the molecular configuration. Such internal free volume, which stems from the paddlewheel-like structure of triptycenes, with three aromatic rings bridged at 120° on a tricyclic ring, is intrinsic to the polymer structure and, as such, it is non-collapsible, similar to the case of inorganic molecular sieves [8,11–17]. Moreover, interlocking effect provided by triptycenes slows down polymer chains dynamics and contributes to maintain the transport properties of these materials stable over time [8]. Several triptycene-containing polymers exhibited performance far above the upper bound and superior resistance to physical aging and plasticization [8]. The superior size sieving ability of triptycene units is essentially ascribable to their "internal free volume", whose size is comparable to that of small molecules, such as CH_4, CO_2 and N_2 [13].

Most of the published work on triptycene-based polymers reports just permeability and selectivity data, with limited fundamental analysis of elemental gas transport properties, such as solubility and diffusivity. Specifically, the role of configurational free volume on elemental transport properties is currently poorly understood. This study aims at filling this gap in the literature. For the first time, a fundamental analysis of gas sorption properties of triptycene-based polymers is presented and several structure-property correlations are identified and discussed. In this study we focus on a novel thermally rearranged polymer, TPBO (trypticene-based polybenzoxazole), prepared from a co-polyimide precursor with controlled triptycene molar content, i.e., triptycene-dianhydride(0.25) − 6FDA(0.75) − 6FAP(1.0) [13]. This material exhibits separation performance far above the upper bound, as well as high resistance to plasticization in the presence of CO_2 [13].

To assess the membrane behavior in realistic conditions, mixed gas sorption behavior was predicted based on the dual mode description of pure gas sorption isotherms. Remarkably, real solubility-selectivity is significantly higher than ideal solubility-selectivity. Finally, water vapor transport was investigated. The latter aspect is of great practical deal, since water vapor is an important component of raw natural gas.

2. Theoretical background

2.1. Small molecule sorption and transport in polymers

Penetrant permeability coefficient through a polymer membrane, $\wp$, is defined as the pressure and thickness normalized flux. The solution-diffusion model relates $\wp$ to the sorption (S) and diffusion ($\bar{D}$) coefficients as follows [18]:

$$\wp = \bar{D} \times S \tag{1}$$

where $\bar{D}$ is the concentration-averaged, effective penetrant diffusion coefficient, and S is the apparent solubility coefficient, which is defined as the ratio C/f, where C is the penetrant concentration in the upstream face of the polymer and f is the upstream penetrant fugacity in the external gas phase. The pure gas (i.e., ideal) selectivity is defined as follows [18]:

$$\alpha_{ij}^{id} = \frac{\wp_i}{\wp_j} = \frac{\bar{D}_i}{\bar{D}_j} \times \frac{S_i}{S_j} = \alpha_D^{id} \times \alpha_S^{id} \tag{2}$$

where α_D^{id} and α_S^{id} are the ideal diffusivity-selectivity and solubility-selectivity, respectively.

The dual mode model is frequently used to correlate and interpret gas and vapor sorption isotherms in glassy polymers [19]. The penetrant concentration in the polymer, C, is assumed as the sum of concentration in the dense, equilibrium polymer phase and that in the non-equilibrium, excess free volume [19]:

$$C = k_D f + \frac{C_H' b f}{1 + b f} \tag{3}$$

where k_D is the Henry's constant, which describes penetrant dissolution in the equilibrium phase, C_H' is the Langmuir sorption capacity, which describes penetrant sorption in the excess free volume, and b is the Langmuir affinity parameter, which quantifies penetrant affinity for the Langmuir sites [19]. Finally, f is the penetrant fugacity in the external gas phase. Fugacity is often used instead of pressure, as it accounts for non-ideal behavior of the gas phase.

Based on the dual mode picture, Paul and Koros developed a theoretical model to describe gas permeability in glassy polymers, known as dual sorption-mobility model [20]. They assigned a non-zero mobility to both the Henry and the Langmuir populations, giving rise to the following expression for gas permeability:

$$\wp = k_D D_D \left(1 + \frac{FK}{1 + bf}\right) \tag{4}$$

where k_D and b are the dual mode parameters retrieved from the analysis of sorption data, f is the upstream penetrant fugacity, $F = D_H/D_D$ and $K = C_H' b/k_D$, where D_D and D_H are the diffusion coefficients of penetrant molecules sorbed in the Henry and Langmuir mode, respectively [20].

Koros extended the dual mode model to gas mixtures [21]. When a glassy polymer is brought in contact with a gas mixture of components i and j, the concentration of species i in the polymer is expressed as follows [21]:

$$C_i = k_{D,i} f_i + \frac{C_{H,i}' b_i f_i}{1 + b_i f_i + b_j f_j} \tag{5}$$

where the fugacity of species i and j is a function of pressure and gas mixture composition (i.e., $f_i = f_i(p, y_i)$). According to Eq. (5), the presence of the second component reduces the concentration of species i in the polymer, due to competitive sorption into the Langmuir sites [21]. Once the dual mode parameters are available for pure gas sorption, the model becomes predictive for mixed gas sorption, provided that no specific penetrant-penetrant and penetrant-polymer interactions take place.

The mixed gas sorption coefficient of species i is defined as follows:

$$S_i^{mix} = \frac{C_i^{mix}(f_i)}{f_i} \tag{6}$$

Based on this definition, the mixed gas (i.e., real) solubility-selectivity is expressed by Eq. (7):

$$\alpha_S = \frac{S_i^{mix}}{S_j^{mix}} \tag{7}$$

To describe the sorption of associating vapors, such as water and alcohols, in glassy polymers, Feng modified the original dual mode model as follows [22]:

$$C = \frac{c_P k A a}{(1 - ka)(1 - ka + Aka)} \tag{8}$$

where C is the vapor concentration in the polymer, a is the vapor activity (i.e., f/f^*, where f^* is the saturation fugacity), c_p represents the sorption capacity of first sorption monolayer, i.e., the sorption capacity of first shell of water molecules interacting directly with the polymer backbone, and A and k are the dimensionless heats of sorption of the first and higher order penetrant layers, respectively [22].

2.2. Clustering

The tendency of penetrant molecules to form clusters can be assessed using the quantitative method developed by Zimm and Lundberg [23]:

$$\frac{G_{11}}{\bar{V}_1} = (\phi_1 - 1)\left[\frac{\partial\left(\frac{a}{\phi_1}\right)}{\partial a}\right]_{T,p} - 1 \quad (9)$$

where G_{11} is the cluster integral, $\bar{V}_1$ is the penetrant partial molar volume, a is the activity and ϕ_1 is the penetrant volume fraction. The quantity $\frac{\phi_1 G_{11}}{\bar{V}_1}$ represents the number of vapor molecules in the cluster in excess to a single molecule. Based on this analysis, clustering takes place when $\frac{\phi_1 G_{11}}{\bar{V}_1}$ is greater than zero [23]. The penetrant volume fraction in the polymer is calculated from sorption data as $\phi = \frac{\frac{CV_1}{22414}}{1+\frac{CV_1}{22414}}$ [24], where C is expressed in cm^3(STP)/cm^3polymer and V_1 is the penetrant molar volume (18 cm^3/mol for water at 35 °C).

2.3. Temperature dependence of solubility

The temperature dependence of gas sorption in polymers is described by a van't Hoff relationship [25,26]:

$$S = S_0 \exp\left(-\frac{\Delta H_S}{RT}\right) \quad (10)$$

where S_0 is a pre-exponential constant and ΔH_S is the enthalpy of sorption. The latter represents the algebraic sum of the condensation enthalpy, ΔH_{cond}, and the mixing enthalpy, ΔH_{mix}. ΔH_{mix} accounts for penetrant-polymer interactions, as well as for the energy needed to open gaps between polymer chains [25]. The concentration dependence of ΔH_S, or isosteric heat of sorption, is expressed as follows [25,26]:

$$\left[\frac{d(\ln p)}{d\left(\frac{1}{T}\right)}\right]_C = \frac{\Delta H_S}{ZR} \quad (11)$$

where Z is the compressibility factor and p is the equilibrium pressure corresponding at each concentration, C.

3. Experimental

3.1. Polymer synthesis, film casting and thermal treatment

Details about precursor synthesis and film casting, as well as thermal conversion to polybenzoxazole are reported in our previous study [13]. For the sake of brevity, they are briefly described in the Supporting Information. Polymer structure and relevant properties are summarized in Table 1.

3.2. Pure gas and vapor sorption measurements

Pure He, N_2, CH_4, CO_2 and C_2H_6 sorption in TPBO was measured up to 32 atm and in the temperature range 5–50 °C using a dual chamber barometric sorption apparatus [27]. Water vapor sorption and diffusion were measured at 35 °C using a separate barometric sorption apparatus [28]. Details are provided in the Supporting Information.

4. Results and discussion

4.1. Gas sorption and dual mode modeling

Pure He, N_2, CH_4, CO_2 and C_2H_6 sorption isotherms in TPBO are shown in Fig. 1 A–E as a function of temperature and penetrant fugacity in the contiguous external gas phase. Fugacity was calculated at each temperature using the Peng-Robinson equation of state [29].

Helium sorption isotherms (cf. Fig. 1A) are fairly linear and exhibit a negligible dependence on temperature. Sorption measurements were repeated at least in duplicate and uncertainty was calculated from standard deviation. As helium is a sparingly soluble gas, the uncertainty associated to helium sorption measurement (± 10%) is higher relative to other penetrants. Helium concentration in TPBO at 30 atm and 35 °C is about 6 cm^3(STP)/cm^3polymer, which is larger than in other glassy polymers, such as HAB-6FDA-TR-450–30 min (3 cm^3(STP)/cm^3 polymer) [30], Teflon® AF2400 (4 cm^3(STP)/cm^3polymer) [30] and Matrimid® (< 1 cm^3(STP)/cm^3 polymer) [30]. This result is ascribable to the presence of triptycene units, which disrupt chain packing and likely host a significant amount of penetrant molecules in their internal free volume [13], as well as to different helium interaction modes with different polymers. For permanent gases, such as He and H_2, the contribution of ΔH_{cond} to the sorption enthalpy is fairly negligible, so $\Delta H_S \cong \Delta H_{mix}$ [27]. However, He is an inert gas and, as such, it is not expected to interact in any special way with the polymer. Moreover, since He kinetic diameter (2.6 Å) is much smaller relative to the internal diameter of triptycene units (4 Å), helium molecules can be accommodated into the configurational free volume of triptycenes without requiring gap opening between polymer chains. Based on these arguments, it is likely that $\Delta H_{mix} \cong 0$, which may justify the lack of temperature dependence of helium sorption. Since experimental isotherms are linear, we did not attempt to describe helium sorption with the dual mode model.

N_2, CH_4, CO_2 and C_2H_6 (cf., Fig. 1B-E) sorption isotherms in the range 5–50 °C are concave to the fugacity axis, according with the dual mode behavior of glassy polymers. Experimental uncertainty was calculated using the error propagation method [31]. Variables taken into account for the error determination are: *i)* the uncertainty on the volume of the loading chamber, *ii)* the uncertainty on the volume of the

Table 1
Structure and relevant chemical-physical properties of TPBO [13].

TPBO structure

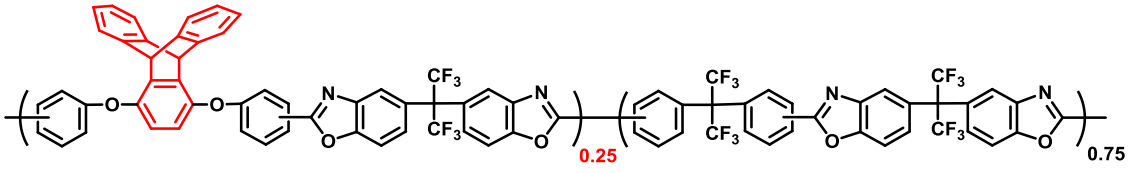

Density[a] (g/cm^3)	Glass transition T[b]	Conversion[c] (%)	D-spacing[d] (Å)
1.393 ± 0.002	no T_g observed up to 400 °C	100	6.8

[a] measured at room temperature using an Archimede's balance.
[b] determined via DSC measurements [13].
[c] conversion was calculated as 100×*actual mass loss*/*theoretical mass loss*. The actual mass loss was calculated from TGA analysis. Theoretical mass loss is the mass loss expected for 100% conversion [13].
[d] measured via WAXD [13].

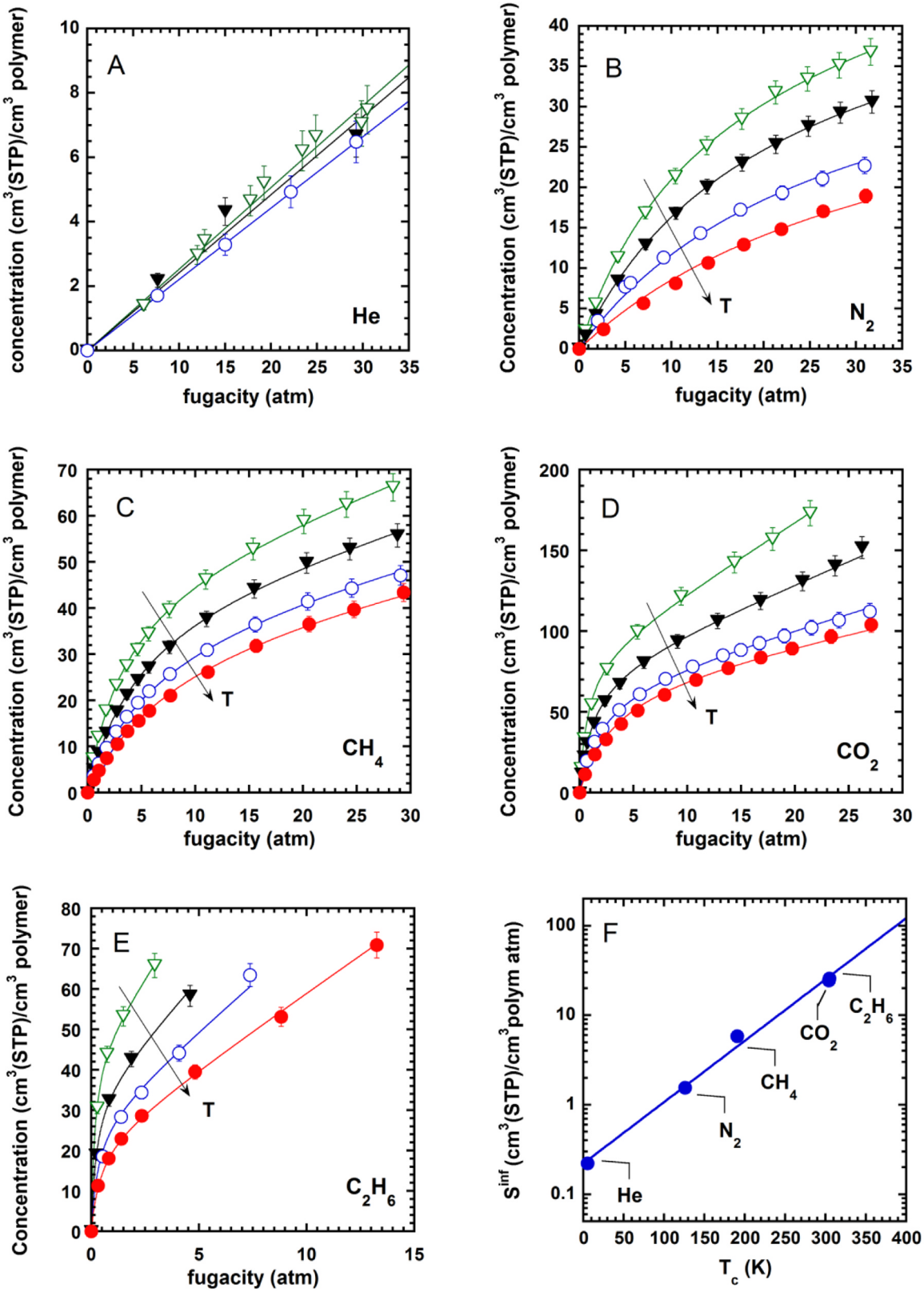

Fig. 1. Sorption isotherms at multiple temperatures in TPBO. A): He; B): N_2; C): CH_4; D): CO_2; E): C_2H_6. Solid red circles: 50 °C; open blue circles: 35 °C; solid black triangles: 20 °C; open green triangles: 5 °C. Continuous lines represent the dual mode fitting to experimental sorption data. F): solubility coefficients at 35 °C and 1 atm as a function of critical temperature.

sorption chamber, *iii)* the uncertainty on the pressure transducers reading, and *iv)* the uncertainty on the polymer density.

At fixed penetrant and external fugacity, sorption increases with decreasing temperature. As shown in Table 2, TPBO exhibits, at 35 °C and 10 atm, higher sorption capacity relative to conventional glassy polymers. For example, gas sorption in TPBO is up to 8% higher than in

Table 2
Solubility coefficient of N_2, CH_4 and CO_2 at 35 °C and 10 atm in several materials suitable for gas separation.

Material	Sorption coefficient (cm^3(STP)/cm^3 atm)			Source
	N_2	CH_4	CO_2	
TPBO	1.17	2.95	7.58	[this study]
Matrimid®	0.30	0.87	3.40	[39]
Polysulfone	0.19	0.67	2.09	[40]
Ultem®	0.18	0.56	2.39	[39]
Zeolite 4 A	5.00	6.65	15.44	[39]
Polycarbonate	0.17	0.40	1.60	[40]
Polyphenylene oxide	/	1.24	2.65	[40]
HAB-6FDA	0.44	1.07	4.0	[32]
TR-450-30 min	1.18	2.80	7.0	[32]
PIM-1	1.66	3.99	9.49	[38]

thermally rearranged polymers obtained from HAB-6FDA polyimide using a similar thermal treatment [32]. This behavior is at least in part due to the presence of triptycene units, which provide extra free volume-based microporosity to accommodate penetrant molecules. Moreover, the sample considered in this study is fully converted to the polybenzoxazole form. In contrast, TR polymers obtained upon treatment of HAB-6FDA at 450 °C for 30 min exhibited a conversion less than 90% [32]. As shown in previous studies [32,33], larger thermal conversion produces larger free volume fractions, which, in turn, enhances gas sorption. d-spacing in TPBO (6.8 Å) is higher than in TR polymers based on HAB-6FDA (< 6.2 Å), which is consistent with the larger sorption capacity exhibited by TPBO. Specifically, the very large CO_2 solubility in TPBO is also ascribable to the presence of polar ether groups on the polymer backbone, which favorably interact with CO_2 molecules [34].

After completing the first CO_2 sorption run at 35 °C, full vacuum was pulled throughout the system for a few hours and a second sorption experiment was run. As shown in Fig. S1, Supporting Information, the two sorption runs overlap within the experimental uncertainty up to a pressure of 10 atm. This result points out that, at least at 35 °C, no permanent matrix conditioning takes place in the presence of CO_2. This result is impressive, considering that CO_2 concentration in TPBO at 30 atm and 35 °C is 112 cm^3(STP)/cm^3polymer. Independent CO_2 pure-gas permeability data confirm that TPBO exhibits very good resistance to swelling and plasticization [13]. This behavior can be ascribed to, at least, four factors, i.e.: *i)* the high rigidity of the polymer backbone, *ii)* the presence of triptycenes, which can possibly accommodate some penetrant molecules without causing matrix swelling (this aspect will be discussed later), *iii)* the interlocking and chain threading effect provided by triptycenes, which act like a cross-link, and *iv)* the $\pi - \pi$ interactions between triptycene aromatic blades.

Ethane sorption isotherms are shown in Fig. 1E. Since ethane molecules (kinetic diameter = 4.44 Å) cannot fit into the triptycene units (internal diameter = 4 Å), we expect that a significant amount of ethane is absorbed in the Henry mode. As discussed later in this paper, this picture is confirmed by the dual mode modeling, so a non-negligible polymer swelling is expected to take place during ethane sorption at high pressure. Therefore, dilation data would be needed to correct sorption isotherms obtained using the barometric technique [35,36]. As shown by Smith et al. [35], exposure to ethane causes non-negligible swelling and plasticization of TR polymers derived from HAB-6FDA and APAF-6FDA at pressure of 10 atm or less. To prevent swelling, we limited our sorption measurements below 10 atm at 5, 20 and 35 °C, and below 15 atm at 50 °C. Work is underway to study the effects of exposure to swelling hydrocarbons at high pressure and will be object of a forthcoming publication. Experimental sorption isotherms exhibit, in the whole range of pressure and temperature investigated, a dual mode behavior. Ethane and carbon dioxide exhibit similar critical temperatures and, consistently, they are absorbed in the polymer to a fairly similar extent (cf., Fig. S2, Supporting Information). However, since C_2H_6 molecule is much larger than CO_2, these penetrants are expected to exhibit a different distribution into the polymer matrix. This aspect will be discussed later in this study.

As shown in Fig. 1F, at fixed temperature, the logarithm of sorption coefficient is linear with critical temperature (i.e., $ln(S) = \alpha + \beta T_C$). The slope of this correlation (i.e., β) at 1 atm and 35 °C is 0.016 K^{-1}, which matches very well with values reported previously for other glassy polymers [37,38]. Gratifyingly, this linear correlation includes helium. Similar results were reported by Smith et al. for He, H_2, N_2, O_2, CH_4 and CO_2 sorption in HAB-6FDA-TR450-30 min. β at 1 atm varies from 0.0158 K^{-1} at 50 °C to 0.0177 K^{-1} at 5 °C. Indeed, sorption of more condensable gases (i.e., gases with larger T_C, such as CO_2 and C_2H_6) increases much more with decreasing temperature than sorption of less condensable gases, which causes an increase in $\beta$with decreasing temperature.

The dual mode model was used to correlate gas sorption data to the polymer structure. As reported by many researchers, different sets of dual mode parameters often describe equally well experimental data [41]. To circumvent this issue, k_D and b were constrained to follow a van't Hoff relationship with temperature, while C'_H was left unconstrained (cf. Table S2, Supporting Information) [42]. The dual mode fitting to experimental sorption isotherms is shown, for each penetrant at each temperature, in Fig. 1-B-E. The complete set of dual mode parameters is reported in Table S1, Supporting Information. At any temperature, the Henry constant, k_D, increases fairly linearly with penetrant critical temperature (i.e., $k_D^{C_2H_6} > k_D^{CO_2} > k_D^{CH_4} > k_D^{N_2}$), despite no constraint was imposed on its values. The Langmuir affinity parameter, b, follows the same behavior. As observed by Koros and Paul in conventional glassy polymers, the Langmuir sorption capacity, C'_H, decreases fairly linearly with increasing temperature [43] (cf. Fig. S3, Supporting Information).

The N_2 and CO_2 Langmuir sorption capacity exhibited by TPBO slightly exceeds that of TR polymers derived from HAB-6FDA [32,42]. This effect is ascribable to the presence of microporous triptycene units, which increase free volume available to accommodate penetrant molecules, as well as to the larger thermal conversion exhibited by TPBO (≅ 100%) relative to HAB-6FDA-TR450-30 min (<90%). In the case of CH_4, C'_H values in TPBO and HAB-6FDA-TR450-30 min are comparable. This result could be due to the natural scattering of the dual mode parameters.

As reported by Luo et al. [13], the diameter of the sphere equivalent to a triptycene unit is approximately 4 Å, which is smaller than the ethane kinetic diameter (i.e., 4.4 Å). As a consequence, ethane molecules cannot be accommodated into the clefts of triptycene units, so they are preferentially sorbed in the Henry mode and in the conformational, excess free volume, like in conventional glassy polymers. This physical picture is confirmed by the dual mode analysis of sorption data. Indeed, at all temperatures investigated, the ethane Langmuir sorption capacity is significantly lower relative to the other penetrants (cf. Table S1, Supporting Information). For example, at 35 °C, C'_H is 68.54 cm^3(STP)/cm^3polymer for CO_2, 40.58 cm^3(STP)/cm^3polymer for N_2 and 27.94 cm^3(STP)/cm^3polymer for C_2H_6. At 35 °C and 10 atm, the Langmuir-to-Henry mode sorption ratio is 0.6 for ethane, 3 for carbon dioxide and 29 for nitrogen.

In the framework of the dual mode model, the excess fractional free volume of glassy polymers, v, can be estimated as follows [44]:

$$v = \frac{\hat{V}_p - \hat{V}_l}{\hat{V}_p} = C'_H\left(\frac{M}{22414}\right)\frac{1}{\rho^*} \tag{12}$$

where M is the penetrant molecular mass, ρ^* is the density of saturated liquid penetrant at the experimental temperature, $\hat{V}_p$ is the polymer specific volume and $\hat{V}_l$ is the specific volume of the equilibrium (i.e., Henry) phase. The TPBO excess free volume was calculated based on CO_2 sorption data at 5 °C. In these conditions, ρ^* = 0.89 g/cm^3 [45],

which gives $\nu = 0.19$. Similar results were obtained at different temperatures. This value is quite high and much larger than for conventional glassy polymers, such as polycarbonate, for which $\nu = 0.04$ [44]. ν was estimated to be 0.16 for HAB-6FDA-TR450-30 min, 0.20 for PTMSP [44] and 0.29 for PIM-1 [37,38]. A comparison between CO_2 sorption isotherms at 35 °C in TPBO and PIM-1, along with the dual mode modeling, is shown in Fig. S4, Supporting Information. PIM-1 exhibits higher gas sorption capacity relative to TPBO, which is consistent with the free volume difference between the two polymers. However, the free volume frozen in PIM-1 is largely conformational (i.e., it originates from the non-equilibrium nature of PIM-1) and, as such, it is subject to collapse over time. Conversely, TPBO contains a significant amount of configurational free volume, which is not collapsible [13].

4.2. Temperature dependence of gas sorption

As shown in Fig. 1, gas sorption in TPBO decreases with increasing temperature, indicating that the sorption process is exothermic. The enthalpy of sorption at infinite dilution, ΔH_s^∞ (i.e., the enthalpy of sorption in the limit of vanishing pressure), was calculated for each penetrant from the slope of the logarithm of infinite dilution sorption coefficient as a function of reciprocal temperature, and its values are shown in Table 3. Infinite dilution sorption coefficients (S^∞) were calculated using the dual mode parameters available for each penetrant at each temperature, according to the formula [19]:

$$S^\infty = k_D + C'_H b \tag{13}$$

To put ΔH_s^∞ data in perspective, they were compared to values reported previously for Teflon®AF2400 [27], a perfluorinated glassy copolymer, HAB-6FDA-TR450-30 min [42] and PIM-1 [38]. Gas sorption in TPBO is more exothermic than in HAB-6FDA-TR450-30 min. Such difference is due to the large free volume provided by hierarchical triptycene units, which can possibly accommodate penetrant molecules in the internal free volume (i.e., in the clefts between the benzene "blades") without requiring the creation of gaps in the polymer matrix. The latter process is, indeed, largely endothermic. Especially, carbon dioxide sorption in TPBO is much more exothermic than in HAB-6FDA-TR450-30 min, which is indicative of thermodynamically favorable interaction between carbon dioxide and TPBO. Indeed, unlike HAB-6FDA-TR450-30 min, TPBO contains ether groups on its backbone, which are known to establish favorable quadrupole interactions with polar CO_2 molecules [34].

Gas sorption in Teflon®AF2400 is much more endothermic than in TPBO [27]. This result is consistent with light gases exhibiting less favorable interaction with fluorinated polymers relative to hydrocarbon-based polymers [27,30]. Moreover, as pointed out by Merkel et al. [27], gas sorption in fluorinated polymers occurs predominantly in the Henry mode, which requires energy to open gaps between polymer chains. For example, ethane sorption in TPBO is significantly more exothermic than in Teflon®AF2400. This result is consistent with TPBO/ethane interaction (hydrocarbon-hydrocarbon type) being more favorable than Teflon®AF2400/ethane interaction (hydrocarbon-fluorocarbon type).

Table 3
Infinite dilution enthalpy of sorption in glassy polymers. The uncertainty on TPBO data was calculated using the error propagation method [31].

	ΔH_s^∞(kJ/mol)			
	TPBO	HAB-6FDA-450-30 min [42]	Teflon® AF2400 [27]	PIM-1 [38]
N_2	− 19.82 ± 1.58	− 15.60	− 11.30	/
CH_4	− 18.55 ± 1.48	− 15.50	− 13.20	− 19.00
CO_2	− 27.72 ± 2.21	− 18.94	− 14.80	− 25.00
C_2H_6	− 27.30 ± 2.20	/	− 12.20	/

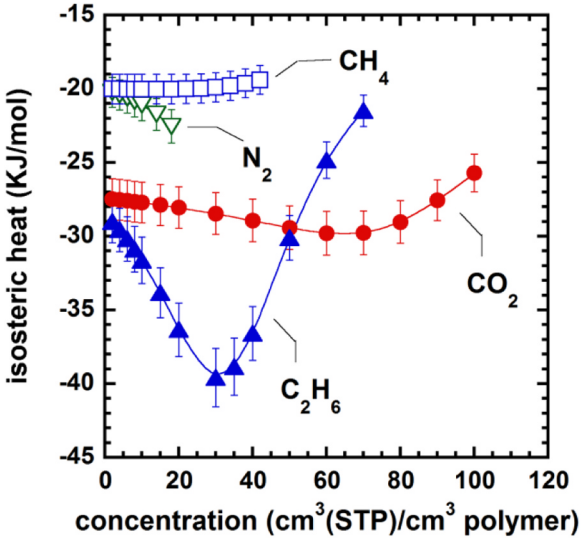

Fig. 2. Enthalpy of sorption as a function of penetrant concentration (i.e., isosteric heat of sorption) in TPBO. Open blue squares: CH_4; open green triangles: N_2; filled red circles: CO_2; filled blue triangles: C_2H_6. Uncertainty was calculated using the error propagation method [31]. Lines are a guide for the eye. (For interpretation of the references to color in this figure legend, the reader is referred to the web version of this article.)

TPBO and PIM-1 exhibit similar enthalpies of sorption at infinite dilution. This similarity likely reflects the microporous structure of these two polymers.

The isosteric heat of sorption, i.e., the concentration dependence of enthalpy of sorption (cf., Fig. 2) discloses a number of fundamental information regarding penetrant distribution in the polymer matrix and polymer-penetrant interactions [25,27]. Isosteric heat of methane and nitrogen sorption in TPBO is, within the experimental uncertainty, fairly independent of concentration, which suggests that sorption occurs essentially in the free volume cavities [27]. This result is confirmed by the dual mode analysis of sorption data, which indicates that sorption in the Langmuir mode exceeds that in the Henry mode. Nitrogen sorption becomes slightly more exothermic with increasing concentration, indicating that polymer-penetrant interaction becomes more thermodynamically favorable at high concentrations. Moreover, methane and nitrogen sorption are energetically equivalent, which indicates that sorption of these penetrants in TPBO changes in a similar fashion with temperature (that is, CH_4/N_2 solubility-selectivity does not change with temperature).

CO_2 sorption in TPBO is largely exothermic, which is consistent with the greater condensability of this penetrant compared to methane and nitrogen. Additionally, favorable CO_2-polymer interactions could be invoked to justify such largely negative ΔH_s. As mentioned above, ether groups on the TPBO backbone are expected to establish favorable interactions with polar CO_2 molecules. ΔH_s is fairly constant, within the experimental uncertainty, up to a CO_2 concentration of 65 cm^3(STP)/cm^3polymer. Indeed, at low-medium pressures, CO_2 molecules are essentially sorbed in the free volume elements, which does not require gap opening between polymer chains. When sorption into the Henry mode becomes significant, a positive (i.e., endothermic) contribution is added to ΔH_s, which justifies the slight increase in ΔH_s. Such endothermic contribution corresponds to the energy needed to open gaps between polymer chains.

Isosteric heat of sorption of C_2H_6 exhibits a prominent increase starting at lower concentration relative to CO_2 (30 vs 65 cm^3(STP)/cm^3polymer, respectively). Since ethane molecules are larger than the internal cleft of triptycenes [13], the configurational free volume does not contribute at all to ethane sorption. Therefore, ethane sorption occurs, at low pressures, in the conformational, excess free volume, as

in conventional glassy polymers. When the excess free volume gets saturated, sorption proceeds prevailingly in the Henry mode. The latter sorption mode is endothermic, since it requires energy to open gaps between polymer chains. This causes a substantial increase in ΔH_{mix} which, in turn, is responsible for the large increase of ΔH_s at concentrations larger than 30 cm^3(STP)/(cm^3 polymer). Moreover, due to the larger molecular size of ethane (kinetic diameter = 4.44 Å) relative to carbon dioxide (kinetic diameter = 3.30 Å) [37], a larger amount of energy is required to accommodate ethane molecules in the Henry sites relative to carbon dioxide, which justifies the much steeper increase of isosteric heat of sorption in the case of ethane. The large decrease of C_2H_6 isosteric heat of sorption at concentration less than 30 cm^3(STP)/(cm^3 polymer) is indicative of strong and favorable polymer-ethane interactions. As reported by several researchers, hydrogen atoms of aliphatic hydrocarbons can establish CH/π interactions with benzene rings [46]. As this polymer is fully aromatic and contains iptycene moieties, strong ethane-TPBO interactions could take place. This hypothesis is also strongly supported by the fact that ethane heat of sorption is much more negative than the heat of condensation (≅ −4.5 KJ/mol). Molecular simulations are underway to clarify this aspect.

4.3. Predicting mixed-gas sorption and solubility-selectivity

Mixed-gas sorption isotherms can be predicted using the dual mode parameters estimated from pure gas sorption data (cf. Eq. (5)). In Fig. 3, predicted mixed CO_2/CH_4 sorption in TPBO is reported for an equimolar CO_2/CH_4 mixture at 35 °C and as a function of total pressure. The mixed gas CO_2/CH_4 solubility-selectivity, α_S, was calculated using Eqs. 6 and 7 and compared with pure gas (i.e., ideal) solubility-selectivity. Ideal solubility-selectivity was calculated using pure gas sorption coefficients at the same fugacity of mixed gas conditions. Fugacities of CO_2 and CH_4 in the gas mixture were calculated using the Peng-Robinson equation of state [29]. The CO_2/CH_4 interaction parameter, k_{ij}, (i.e., 0.09) was taken from literature sources [29].

Mixed gas solubility is depressed relative to single gas solubility. This behavior is attributed to competitive sorption into the Langmuir sites [21]. However, as shown in Fig. 3B-C, CH_4 solubility is depressed much more than CO_2 solubility, which is consistent with CO_2 being a more condensable gas than CH_4. In Fig. 3A, the experimentally determined ideal CO_2/CH_4 solubility-selectivity at 35 °C is compared to mixed gas solubility-selectivity predicted by the dual mode model as a function of total pressure. Interestingly, mixed gas CO_2/CH_4 solubility-selectivity (α_S) is significantly larger than ideal solubility-selectivity (α_S^{id}). This difference becomes remarkable at high pressure, where α_S is approximately twice α_S^{id}. This result is qualitatively consistent with experimental mixed gas solubility-selectivity data reported by Story et al. [47], Raharjo et al. [48] and Vopicka et al. [49] for PPO, PTMSP and PIM-1, respectively. Real CO_2/CH_4 solubility-selectivities for some high performance polymers are compared in Table 4. Interestingly, at 35 °C, TPBO exhibits higher mixed gas CO_2/CH_4 solubility-selectivity relative to other thermally rearranged polymers and PTMSP. Noteworthy, TPBO and PIM-1 exhibit similar mixed gas CO_2/CH_4 solubility-selectivity.

Real CO_2/CH_4 solubility-selectivity increase with decreasing temperature (cf., Fig. 3D). Such behavior is consistent with the analysis of heat of sorption presented in Section 4.2. Indeed, based on Eq. (10), the temperature dependence of solubility-selectivity is expressed as follows:

$$\alpha_{ij}(T) = \frac{S_{0,i}}{S_{0,j}} \exp\left(-\frac{\Delta H_{s,i} - \Delta H_{s,j}}{RT}\right) \quad (14)$$

Since CO_2 sorption is more exothermic than CH_4 sorption, Eq. (14) predicts that CO_2/CH_4 solubility-selectivity increases with decreasing temperature. In contrast, CO_2/CH_4 solubility-selectivity in thermally rearranged polymers based on HAB-6FDA did not change with temperature [42]. This difference makes TPBO a more flexible material than HAB-6FDA-TR450-30 min, since its performance can be modulated by changing the operative conditions.

As shown in Fig. S7-A, Supporting Information, experimental CH_4/N_2 solubility-selectivity is barely affected by temperature. This result is consistent with CH_4 and N_2 exhibiting essentially the same enthalpy of sorption. CO_2/N_2 solubility-selectivity is reported in the Supporting Information (cf. Figs. S6 and S7).

4.4. Diffusion coefficients

Concentration-averaged diffusion coefficients in TPBO at 35 °C were calculated through Eq. (1), coupling sorption data from this study with N_2, CH_4 and CO_2 permeability data at 35 °C and below 10 atm from ref. [13] (cf. Table 5). Interestingly, N_2, CH_4 and CO_2 diffusion coefficients in TPBO are larger than in thermally rearranged polymers derived from HAB-6FDA (cf. Table 5) [33]. This result is consistent with the larger free volume exhibited by TPBO (ν = *0.19*) relative to HAB-6FDA-TR450-30 min (ν = *0.16*, cf. Section 4.1).

The ideal CO_2/CH_4 perm-selectivity exhibited by TPBO exceeds by 33% that of HAB-6FDA-TR450-30 min at 10 atm and 35 °C [33]. As expected, due to the ultrafine microporosity of triptycene units, which enables for superior size-sieving ability, the overall selectivity in TPBO is dominated by the diffusion contribution (cf. Table 5). Interestingly, TPBO exhibits much larger CO_2/CH_4 diffusivity-selectivity relative to conventional polymer membranes for gas separation, such as cellulose acetate (cf. Table 5) [51]. Again, this result is indicative of superior size-sieving ability of iptycene-based polymers. In contrast, cellulose acetate exhibits larger solubility-selectivity relative to TPBO. Overall, the ideal CO_2/CH_4 perm-selectivities shown by TPBO and cellulose acetate are very close (29 vs 32, respectively), while the former polymer is much more permeable.

Finally, TPBO exhibits a CO_2/CH_4 solubility-selectivity similar to that of PIM-1, but a much larger diffusivity-selectivity, despite sorption, diffusion and permeation coefficients in PIM-1 are larger relative to those in TPBO. Indeed, PIM-1 exhibits a larger free volume relative to TPBO, but the ultrafine microporosity of triptycene units in TPBO enables for superior size-sieving ability.

Diffusion coefficients in TPBO at 35 °C increase with increasing penetrant concentration in the polymer (cf. Fig. 4), which could be explained by invoking matrix plasticization. However, light gases such as nitrogen and methane, as well as carbon dioxide below 10 atm, are unlike to plasticize this highly rigid polymer. The same behavior was reported by Paul et al. for PIM-1 [37,38], where N_2 and CH_4 diffusion coefficients also increased with increasing penetrant concentration. The dual sorption-mobility model helps understand the fundamental origin of this behavior [20]. As expected from Eq. (4), permeability exhibits a nice linear trend versus $1/(1+bf)$ (cf. Fig. S8, Supporting Information), from which F, D_D and D_H were estimated [20]. Specifically, F was estimated from the slope of the interpolating line, and D_D was estimated from the intercept. In the dual sorption-mobility model, D_D and D_H are assumed independent on concentration or fugacity [20]. Taken individually, D_D and D_H in TPBO are smaller than in PIM-1 [37], but much larger than in conventional glassy polymers for gas separation, such as polysulfone [52] (cf. Table 6).

Interestingly, the F ratio (i.e., D_H/D_D) calculated for N_2, CH_4 and CO_2 in TPBO is lower than in any other polymer [37] (cf. Table 6). Specifically, diffusion coefficients in the Henry mode of TPBO, D_D, exceed those in the Langmuir sites, D_H, by 2 orders of magnitude. This result indicates that the Langmuir population trapped in the free volume of TPBO is endowed with a very low mobility, which is consistent with the high rigidity of TPBO backbone and with the fact that the size of internal free volume of triptycene units is comparable to the penetrant molecular size. The large difference between D_D and D_H justifies the increase in diffusion coefficient with increasing penetrant concentration in the polymer. Indeed, at low fugacities (i.e., at low concentrations) penetrant sorption occurs essentially in the Langmuir

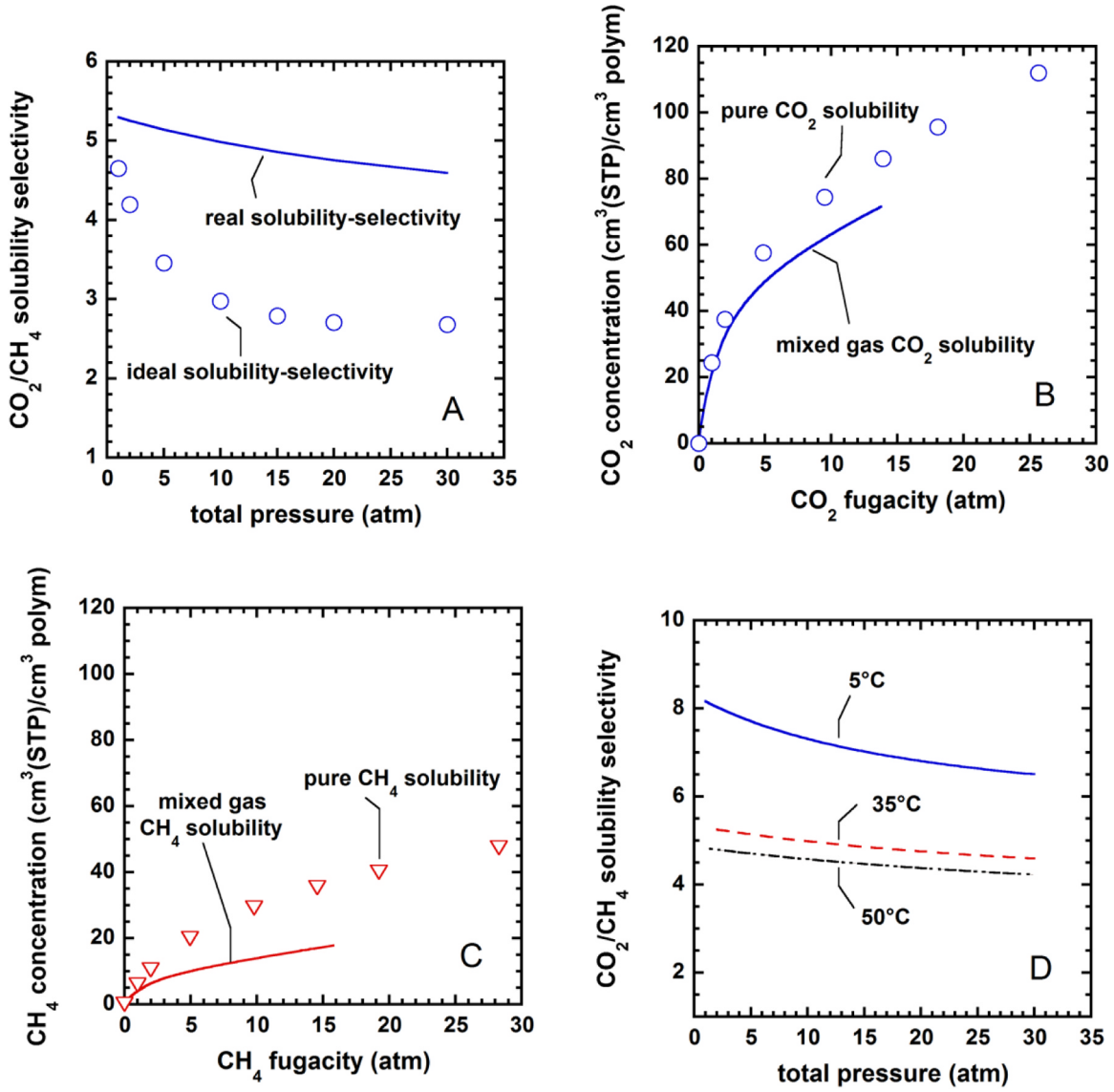

Fig. 3. A) Ideal vs. real CO_2/CH_4 solubility-selectivity at 35 °C for TPBO. Open circles are experimental data and the line is the prediction of the dual mode model for mixed gas sorption. B) Pure and mixed gas CO_2 solubility in TPBO at 35 °C. Open circles are experimental data and the line is the prediction of the dual mode model for mixed gas sorption. C) Pure and mixed gas CH_4 solubility in TPBO at 35 °C. Open triangles are experimental data the line is the prediction of the dual mode model for mixed gas sorption. Mixed gas sorption isotherms and solubility-selectivity were predicted assuming a mixture 50:50% mol CO_2/CH_4. D) CO_2/CH_4 real solubility-selectivity for a mixture 50:50 mol% CO_2/CH_4 as a function of temperature and pressure, calculated using the dual mode model for mixed gas sorption.

Table 4
Mixed gas, CO_2/CH_4 solubility-selectivity at 35 °C in two thermally rearranged polymers, PTMSP and PIM-1. Data refer to a 50:50 mol% CO_2/CH_4 mixture.

	Mixed gas CO_2/CH_4 solubility-selectivity at 35 °C		
Polymer	1 atm	15 atm	30 atm
TPBO[a]	5.30	4.86	4.60
HAB-6FDA-TR450-30 min[a]	4.5	3.5	3
PTMSP[b]	2.2	2.5	4
PIM-1[b]	5.5	/	/

[a] calculated values (using the dual mode model).
[b] experimental values [49,50].

mode. As shown before, the Langmuir population has little mobility in TPBO. As concentration increases, an increasing amount of penetrant is absorbed into the Henry mode. Since the Henry population is endowed with much larger mobility relative to the Langmuir population, diffusion coefficients have to increase with increasing penetrant concentration in the polymer [20]. The same behavior was observed by Paul et al. in PIM-1 [37], which, like TPBO, exhibits a highly rigid and microporous structure. Therefore, the increase in diffusion coefficient with concentration is not indicative of matrix plasticization, but is correlated to the polymer structure. The very low mobility of the Langmuir population in TPBO helps explaining the significant decrease in diffusivity with increasing the molar concentration of triptycene units reported by Luo et al. [13]. As shown in the insert in Fig. 4, diffusion coefficients at 10 atm 35 °C decrease linearly with the square of penetrant kinetic diameter, which is consistent with the phenomenological model proposed by Meares [53].

4.5. Water vapor sorption and transport

Water vapor sorption isotherm in TPBO at 35 °C is reported in Fig. 5A as a function of penetrant activity. To put our data in perspective, they were compared with water vapor sorption in two polybenzoxazoles without triptycene units, namely p-HAB-6FDA-TR450 and

Table 5
Gas permeability and diffusion coefficients in TPBO, HAB-6FDA-TR450-30 min [33], cellulose acetate [51] and PIM-1 [38]. Uncertainty of diffusivity data for TPBO was calculated using the error propagation method [31] and it is less than 7%. For TPBO, HAB-6FDA-TR450-30 min and PIM-1 data are provided at 10 atm and 35 °C. For cellulose acetate, data are provided at 1 atm and 35 °C.

	TPBO	*HAB-6FDA-TR450–30 min*	*Cellulose acetate*	*PIM-1*
$\wp_{CH_4}$ (Barrer)	36.5 ± 0.79	19.7 ± 0.4	0.15	388.5
D_{CH_4} (cm^2/s)	(9.25 ± 0.5)×10^{-8}	(5.0 ± 0.2)×10^{-8}	1.9×10^{-8}	7.3×10^{-7}
$\wp_{CO_2}$(Barrer)	1042 ±24	421.6 ±10	4.8	4419
D_{CO_2}(cm^2/s)	(1.0 ± 0.07)×10^{-6}	(4.4 ± 0.1)×10^{-7}	1.8×10^{-8}	3.6×10^{-6}
$\wp_{N_2}$(Barrer)	56.9 ± 1	25.3 ± 0.6	0.15	288
D_{N_2}(cm^2/s)	(3.68 ± 0.2)×10^{-7}	(1.60 ± 0.1)×10^{-7}	/	1.3×10^{-6}
$\alpha^{id}_{CO_2/CH_4}$	28.6	21.4	32	11.40
$\alpha^{id}_{S,CO_2/CH_4}$	2.63	2.43	8.2	2.33
$\alpha^{id}_{D,CO_2/CH_4}$	10.86	8.8	4.0	4.86

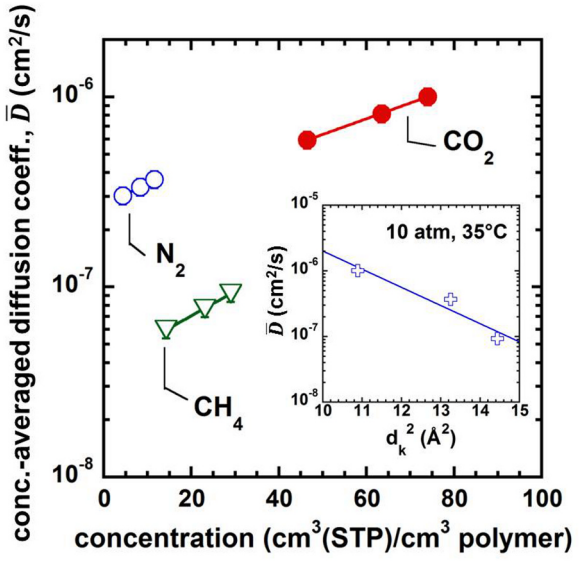

Fig. 4. N_2, CH_4 and CO_2 diffusion coefficients at 35 °C in TPBO as a function of penetrant concentration. Lines were drawn to guide the eye. The insert shows diffusion coefficients at 35 °C and 10 atm as a function of square kinetic diameter, d_k^2. Uncertainty of diffusivity data [31] was lower than 7%. Error bars are too small to show.

Table 6
Dual sorption-mobility parameters at 35 °C for TPBO, PIM-1 [38] and polysulfone [52].

Material	Penetrant	*F*	D_D (cm^2/s)	D_H (cm^2/s)
TPBO	N_2	0.004	3.00×10^{-6}	1.26×10^{-8}
	CH_4	0.005	5.13×10^{-7}	2.33×10^{-9}
	CO_2	0.046	3.66×10^{-6}	1.70×10^{-7}
PIM-1	N_2	0.030	4.37×10^{-6}	1.31×10^{-7}
	CH_4	0.010	4.77×10^{-6}	4.77×10^{-8}
	CO_2	0.054	1.22×10^{-5}	6.57×10^{-7}
Polysulfone	N_2	0.566	9.30×10^{-9}	5.25×10^{-9}
	CH_4	0.174	6.90×10^{-9}	1.20×10^{-9}
	CO_2	0.118	4.53×10^{-8}	5.35×10^{-9}

m-HAB-6FDA-TR450 [54,55]. This comparison is made at fixed temperature and the same duration of thermal treatment (i.e., all samples were thermally rearranged at 450 °C for 30 min). Water vapor sorption in TPBO is about twice that in m-HAB-6FDA-TR450 and largely exceeds that in p-HAB-6FDA-TR450. While differences in water sorption capacity between the latter two samples are due to differences in fractional free volume, the larger water vapor solubility in TPBO is due to a combination of structural and chemical-physical effects. First, unlike p-HAB-6FDA-TR450 and m-HAB-6FDA-TR450, TPBO exhibits polar ether groups on the polymer backbone, which can potentially form hydrogen bonds with water molecules. This feature makes the latter material much more hydrophilic than previously reported TR polymers. Moreover, the microporosity induced by triptycene units provides room to accommodate penetrant molecules. As shown in Section 4.1, TPBO exhibits larger excess free volume relative to TR polymers based on HAB-6FDA polyimide.

Interestingly, water vapor sorption does not induce any permanent polymer conditioning in TPBO. After the first sorption run, full vacuum was pulled throughout the system for a few hours at 35 °C and a second sorption experiment was run. The two sorption isotherms exhibit excellent agreement, which rules out occurrence of long lasting conditioning (cf. Fig. 5A). This result is remarkable, as water vapor sorption induces severe plasticization in 6FDA-based polyimides at activities of about 0.3 [56].

The new dual mode sorption model developed by Feng [22] was used to describe water vapor sorption in TPBO. The best fit values of the three model parameters, c_p, k and A are reported in Table 7.

c_p represents the sorption capacity of the first hydration layer. Its value for TPBO, 31.3 cm^3(STP)/(cm^{3}polymer), is much higher than for TR polymers based on HAB-6FDA [54] (i.e., 9.5 cm^3(STP)/cm^3 polymer). This result reflects the greater hydrophilicity of TPBO relative to pHAB-6FDA-TR-450-30 min, likely due to the presence of ether groups on its backbone. Moreover, the c_p value for TPBO is comparable to total water concentration in the polymer, suggesting that the vast majority of water is available as a single hydration shell (i.e., clustering of water molecules is negligible). k and A values for TPBO are significantly larger than those exhibited by TR polymers derived from HAB-6FDA [54], which confirms the higher hydrophilicity of TPBO. Moreover, c_p and A are much larger than k, which confirms that water clustering is negligible in the investigated activity range [57].

Water vapor sorption kinetics exhibit Fickian behavior [58] (cf., Fig. S9, Supporting Information), from which the concentration-averaged diffusion coefficients were estimated. Water vapor diffusion coefficients in TPBO at 35 °C exhibit a constant trend as a function of activity (cf. Fig. 5B). Generally speaking, the concentration (or activity) dependence of vapor diffusion coefficient in polymers is ruled by the interplay between matrix swelling and penetrant clustering [59]. Indeed, matrix swelling would promote faster penetrant diffusion in the polymer, while penetrant clustering would act in the opposite direction. While a molecular investigation of this phenomenon would require a dedicated spectroscopic study [60], here we can use a simplified quantitative argument to assess the role of swelling and clustering. Specifically, the Zimm-Lundberg integral [23] for the system TPBO-water is lower than zero over the investigated activity range (cf. Fig. S10, Supporting

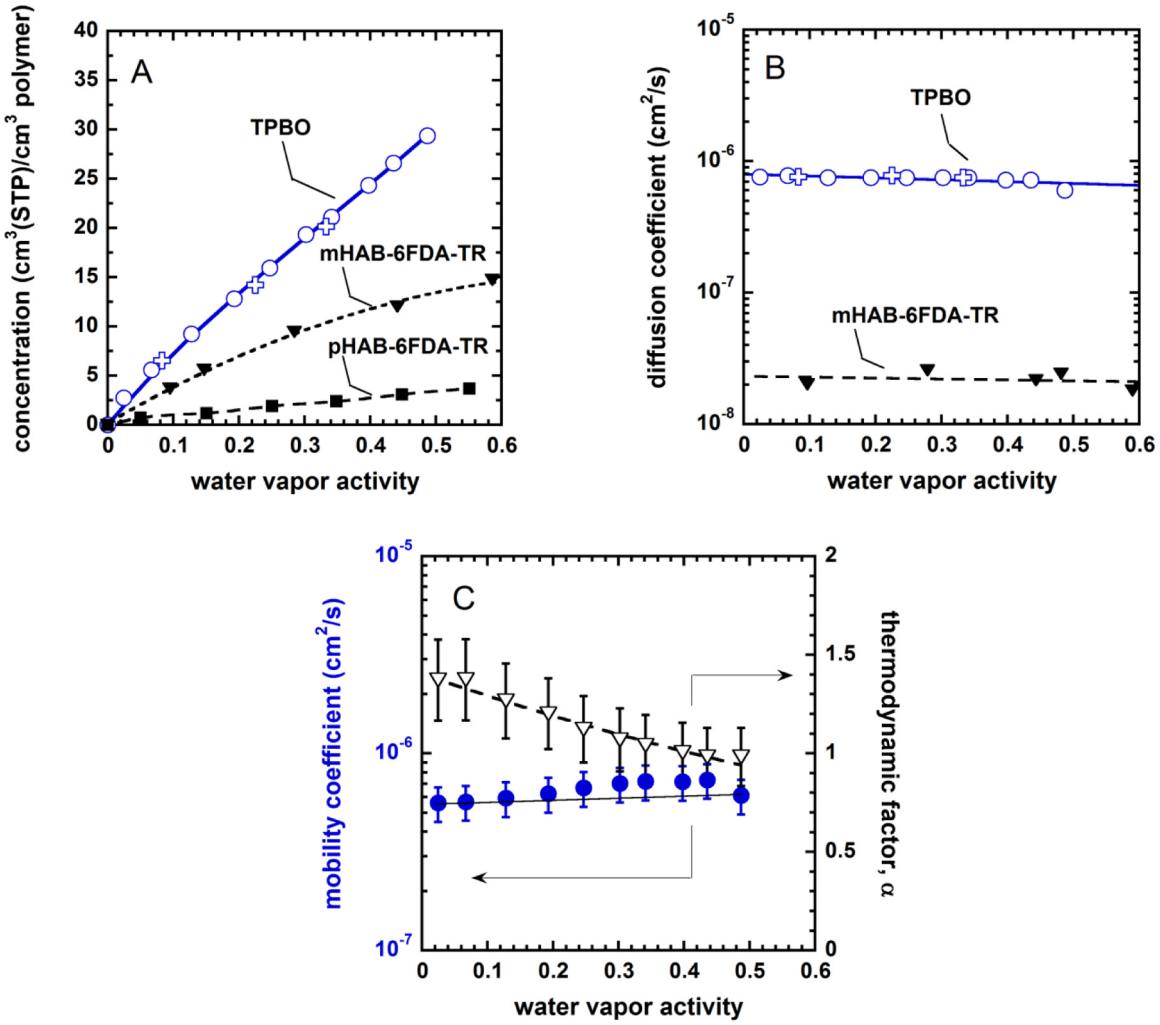

Fig. 5. A) Water vapor sorption isotherms in TPBO at 35 °C. Blue open circles represent sorption data obtained during the first sorption run, and blue crosses represent sorption data obtained during the second sorption run. The continuous line represents the Feng's model fitting to experimental sorption data [22]. For the sake of comparison, water vapor sorption at 35 °C in m-HAB-6FDA-TR450 and p-HAB-6FDA-TR450 were reported [54,55]. B) Water vapor diffusion coefficient at 35 °C in TPBO and m-HAB-6FDA-TR450. Blue open circles represent diffusivity data obtained during the first sorption run, and blue crosses represent diffusivity data obtained during the second sorption run. For the sake of comparison, water vapor diffusion coefficients at 35 °C in m-HAB-6FDA-TR450 were reported [55]. Lines are a guide for the eye. C) Water mobility coefficient and thermodynamic factor at 35 °C, as calculated from Eq. (15). Uncertainty of L and α was calculated using the error propagation method, based on uncertainty of sorption and diffusion coefficients and activity [31]. Lines were drawn to guide the eye. (For interpretation of the references to color in this figure legend, the reader is referred to the web version of this article.)

Table 7
Feng parameters at 35 °C, as retrieved by fitting water vapor experimental sorption data to Eq. (8). For the sake of comparison, values for pHAB-6FDA-TR-450–30 min are also reported.

	c_p (cm^3(STP)/cm^3polymer)	A	k
TPBO[a]	31.30 ± 5.1	4.02 ± 0.6	0.64 ± 0.10
pHAB-6FDA-TR-450-30 min[b]	9.50 ± 1.1	2.8 ± 0.4	0.25 ± 0.08

[a] Uncertainty on the dual mode parameters was calculated using the error propagation method [31].
[b] from ref. [54].

Information), which would rule out the occurrence of water clustering. This result is consistent with the shape of water vapor sorption isotherm, which does not exhibit any upturn, as well as with outcomes of the Feng's model [22]. Water sorption in TPBO differs substantially from that in other rigid glassy polymers, such as 6FDA-6FpDA polyimide, where onset of water clustering was detected at activities as low as 0.3 [56,61]. Based on the Zimm-Lundberg analysis [23], occurrence of polymer swelling and plasticization can be also ruled out. Indeed, in the absence of clustering, polymer swelling would cause an increase of water vapor diffusion coefficient as a function of activity [1].

Water vapor diffusion coefficients in TPBO are one order of magnitude larger relative to those in m-HAB-6FDA-TR450 [54,55]. This behavior is consistent with the larger free volume exhibited by TPBO (19%) relative to mHAB-6FDA-TR450 (16%).

When the concentration difference (in place of chemical potential difference) across the membrane is assumed as the driving force for penetrant transport, the diffusion coefficient, $\bar{D}$, is the product of a mobility coefficient, L, which accounts for the frictional resistance offered by the polymer to penetrant diffusion, and a thermodynamic factor, α, which accounts for polymer-penetrant interactions [28,62]. In case of ideal mixing, $\alpha = 1$. If polymer-penetrant interactions are thermodynamically favorable, α is greater than one. Finally, $\alpha < 1$ indicates unfavorable polymer-penetrant interactions. L (i.e., the diffusion coefficient corrected for thermodynamic non-idealities) and α can be calculated from sorption and diffusion data as follows [28,62]:

$$\alpha = \frac{1}{RT}\frac{\partial \mu_1}{\partial \ln(\omega_1)} = \frac{\ln\left(\frac{a_1^{in}}{a_1^{fin}}\right)}{\ln\left(\frac{\omega_1^{in}}{\omega_1^{fin}}\right)} \quad (15)$$

where ω is the penetrant mass fraction in the polymer, $\mu$is the penetrant chemical potential (subscript 1 stands for the penetrant species), and superscripts *in* and *fin* indicate activity and concentration at the beginnings and at the end of the *i-th* sorption step, respectively. In Fig. 5C, L and α are reported as a function of water activity. The mobility coefficient is constant, within the experimental uncertainty, with penetrant activity, which confirms the analysis of diffusion coefficients presented earlier. The thermodynamic factor changes between 1.3 and 1 over the activity range investigated and indicates that polymer-penetrant interactions are slightly more favorable than expected based on the hypothesis of ideal mixing. The slight change of α over the activity range investigated is within the experimental uncertainty and, as such, it is not statistically significant, so we didn't attempt to explain it on fundamental basis. The relevant finding is that α is larger than 1, which is consistent with the picture that water molecules interact favorably with TPBO, likely by forming hydrogen bonds with ether groups on the polymer backbone.

5. Conclusions

The fundamental transport properties of a novel thermally rearranged copolymer containing triptycene units were reported and discussed. He, N_2, CH_4 and CO_2 sorption coefficients in TPBO were larger than in other glassy polymers, but lower relative to PIM-1. Despite the very high gas sorption capacity, TPBO exhibits good resistance to conditioning and plasticization in the presence of carbon dioxide and water vapor, as confirmed by parallel permeability experiments. This fact reflects the high polymer rigidity, as well as the microporous structure of triptycene units, which likely take up a portion of penetrant molecules without causing matrix swelling. The temperature dependence of gas sorption was investigated. The analysis of sorption enthalpies pointed out a certain CO_2-philicity of TPBO, likely due to the presence of polar ether groups on the polymer backbone. Mixed gas CO_2/CH_4 solubility-selectivity predicted by the dual mode model is higher than ideal solubility-selectivity. Moreover, solubility-selectivity is similar to that exhibited by other high performance materials, but lower relative to that of cellulose acetate.

The dual mobility analysis of diffusion coefficients indicated that the high polymer rigidity slows down diffusion of penetrant molecules trapped in the Langmuir sites. Gas diffusivity and permeability coefficients in TPBO are larger than in other glassy polymers, except PIM-1, and the overall membrane performance largely exceeds the 2008 Upper bound. As expected, based on the ultrafine microporosity of triptycene units which enables superior size-sieving ability, the overall selectivity in TPBO is dominated by the contribution of diffusivity. Diffusivity-selectivity exhibited by TPBO is larger relative to other advanced polymeric materials.

Finally, water vapor sorption and diffusion was investigated at 35 °C. Ether groups on the polymer backbone make this polymer more hydrophilic than previously reported TR polymers. Moreover, the large free volume provided by triptycenes enhances water vapor diffusivity by one order of magnitude relative to TR polymers obtained from HAB-6FDA polyimide.

Acknowledgments

MG acknowledges the University of Oklahoma, Office of Vice Provost, for the financial support. VL acknowledges the University of Naples Federico II for supporting his stay at the University of Oklahoma. RG acknowledges the financial support from the National Science Foundation under the cooperative agreement No. EEC-1647722, an Engineering Research Center for the Innovative and Strategic Transformation of Alkane Resources (CISTAR).

Appendix A. Supplementary material

Supplementary data associated with this article can be found in the online version at doi:10.1016/j.memsci.2018.12.054.

References

[1] M. Galizia, W.S. Chi, Z.P. Smith, T.C. Merkel, R.W. Baker, B.D. Freeman, Macromolecules 50 (2017) 7809–7843.
[2] L.M. Robeson, Correlation of separation factor versus permeability for polymeric membranes, J. Membr. Sci. 62 (1991) 165–185.
[3] L.M. Robeson, The upper bound revisited, J. Membr. Sci. 320 (2008) 390–400.
[4] H.B. Park, C.H. Jung, Y.M. Lee, A.J. Hill, S.J. Pas, S.T. Mudie, E. Van Wagner, B.D. Freeman, D.J. Cookson, Polymers with cavities tuned for fast selective transport of small molecules and ions, Science 318 (2007) 254–258.
[5] P.M. Budd, B.S. Ghanem, S. Makhseed, N.B. McKeown, K.J. Msayib, C.E. Tattershall, Polymers of intrinsic microporosity (PIMs): robust, solution-processable, organic nanoporous materials, Chem. Comm. 2 (2004) 230–231.
[6] M. Carta, R. Malpass-Evans, M. Croad, Y. Rogan, J.C. Jansen, P. Bernardo, F. Bazzarelli, N.B. McKeown, An efficient polymer molecular sieve for membrane gas separations, Science 339 (2013) 303–307.
[7] Y. Huang, D.R. Paul, Physical aging of thin glassy polymer films monitored by gas permeability, Polymer 45 (2004) 8377–8393.
[8] J.R. Weidman, R. Guo, The use of Iptycenes in rational macromolecular design for gas separation membrane applications, Ind. Eng. Chem. Res. 56 (2017) 4220–4236.
[9] R.R. Tiwari, J. Jin, B.D. Freeman, D.R. Paul, Physical aging, CO_2 sorption and plasticization in thin films of polymer with intrinsic microporosity (PIM-1), J. Membr. Sci. 537 (2017) 362–371.
[10] Y.J. Cho, H.B. Park, High performance polyimide with high internal free volume elements, Macromol. Rapid Commun. 32 (2011) 579–586.
[11] J.R. Weidman, S. Luo, Q. Zhang, R. Guo, Structure manipulation in triptycene-based polyimides through main chain geometry variation and its effect on gas transport properties, Ind. Eng. Chem. Res. 56 (2017) 1868–1879.
[12] S. Luo, J.R. Wiegand, B. Kazanowska, C.M. Doherty, K. Konstas, A.J. Hill, R. Guo, Finely tuning the free volume architecture in iptycene-containing polyimides for highly selective and fast hydrogen transport, Macromolecules 49 (2016) 3395–3405.
[13] S. Luo, Q. Zhang, L. Zhu, H. Lin, B.A. Kazanowska, C.M. Doherty, A.J. Hill, P. Gao, R. Guo, Highly selective and permeable microporous polymer membranes for hydrogen purification and CO_2 removal from natural gas, Chem. Mater. 30 (2018) 5322–5332.
[14] A. Fuoco, B. Comesaña-Gándara, M. Longo, E. Esposito, M. Monteleone, I. Rose, C.G. Bezzu, M. Carta, N.B. McKeown, J.C. Jansen, Temperature dependence of gas permeation and diffusion in triptycene-based ultrapermeable polymers of intrinsic microporosity, ACS Appl. Mater. Interfaces 10 (2018) 36475–36482.
[15] M. Carta, M. Croad, R. Malpass-Evans, J.C. Jansen, P. Bernardo, G. Clarizia, K. Friess, M. Lanč, N.B. McKeown, Triptycene induced enhancement of membrane gas selectivity for microporous Tröger's base polymers, Adv. Mater. 26 (2014) 3526–3531.
[16] M. Lanč, K. Pilnáček, C.R. Mason, P.M. Budd, Y. Rogan, R. Malpass-Evans, M. Carta, B. Comesana-Gandara, N.B. McKeown, J.C. Jansen, O. Vopička, K. Friess, Gas sorption in polymers of intrinsic microporosity: the difference between solubility coefficients determined via time-lag and direct sorption experiments, J. Membr. Sci. 570–571 (2019) 522–536.
[17] Z.X. Low, P.M. Budd, N.B. McKeown, D.A. Patterson, Gas permeation properties, physical aging, and its mitigation in high free volume glassy polymers, Chem. Rev. 118 (2018) 5871–5911.
[18] J.G. Wijmans, R.W. Baker, The solution-diffusion model: a review, J. Membr. Sci. 107 (1995) 1–21.
[19] W.J. Koros, A.H. Chan, D.R. Paul, Sorption and transport of various gases in polycarbonate, J. Membr. Sci. 2 (1977) 165–190.
[20] D.R. Paul, W.J. Koros, Effect of partially immobilizing sorption on permeability and the diffusion time lag, J. Polym. Sci: Polym. Phys. Ed. 14 (1976) 675–685.
[21] W.J. Koros, Model for sorption of mixed gases in glassy polymers, J. Polym. Sci: Polym. Phys. Ed. 18 (1980) 981–992.
[22] H. Feng, Modeling of vapor sorption in glassy polymers using a new dual mode sorption model based on multilayer sorption theory, Polymer 48 (2007) 2988–3002.
[23] B.H. Zimm, J.L. Lundberg, Sorption of vapors by high polymers, J. Phys. Chem. 60 (1956) 425–428.
[24] A. Singh, B.D. Freeman, I. Pinnau, Pure and mixed gas acetone/nitrogen permeation properties of polydimethylsiloxane [PDMS], J. Polym. Sci. B: Polym. Phys. 36 (1998) 289–301.
[25] M. Galizia, C. Daniel, G. Guerra, G. Mensitieri, Solubility and diffusivity of low molecular weight compounds in semi-crystalline poly-(2,6-dimethyl-1,4-phenylene) oxide: the role of the crystalline phase, J. Membr. Sci. 443 (2013) 100–106.
[26] W.J. Koros, D.R. Paul, G.S. Huvard, Energetics of gas sorption in glassy polymers, Polymer 20 (1979) 956–960.
[27] T.C. Merkel, V.I. Bondar, K. Nagai, B.D. Freeman, Yu.P. Yampolskii, Gas sorption, diffusion and permeation in Poly(2,2-bis(trifluoromethyl) – 4,5-difluoro-1,3-

dioxole-co-tetrafluoroethylene, Macromolecules 32 (1999) 8427–8440.
[28] M. Galizia, M.G. De Angelis, E. Finkelshtein, Yu.P. Yampolskii, G.C. Sarti, Sorption and transport of hydrocarbons and alcohols in addition-type poly(trimethyl silyl norbornene). I: experimental data, J. Membr. Sci. 385–386 (2011) 141–153.
[29] S.I. Sandler, Chemical and Engineering Thermodynamics, 3rd ed., Wiley, New York, 1999.
[30] Z.P. Smith, R.R. Tiwari, M.E. Dose, K.L. Gleason, T.M. Murphy, D.F. Sanders, G. Gunawan, L.M. Robeson, D.R. Paul, B.D. Freeman, Influence of diffusivity and sorption on helium and hydrogen separations in hydrocarbon, silicon, and fluorocarbon-based polymers, Macromolecules 47 (2014) 3170–3184.
[31] P.R. Bevington, D.K. Robinson, Data Reduction and Error Analysis for the Physical Sciences, 3rd ed., McGraw-Hill, Boston, 2003.
[32] Z.P. Smith, D.F. Sanders, C.P. Ribeiro, R. Guo, B.D. Freeman, D.R. Paul, J.E. McGrath, S. Swinnea, Gas sorption and characterization of thermally rearranged polyimides based on 3,3′-dihydroxy-4,4′-diamino-biphenyl (HAB) and 2,2′-bis-(3,4-dicarboxyphenyl) hexafluoropropane dianhydride (6FDA), J. Membr. Sci. 415–416 (2012) 558–567.
[33] D.F. Sanders, Z.P. Smith, C.P. Ribeiro, R. Guo, J.E. McGrath, D.R. Paul, B.D. Freeman, Gas permeability, diffusivity, and free volume of thermally rearranged polymers based on 3,3′-dihydroxy-4,4′-diamino-biphenyl (HAB) and 2,2′-bis-(3,4-dicarboxyphenyl) hexafluoropropane dianhydride (6FDA), J. Membr. Sci. 409–410 (2012) 232–241.
[34] V.I. Bondar, B.D. Freeman, I. Pinnau, Gas sorption and characterization of poly (ether-b-amide) segmented block copolymers, J. Polym. Sci. B: Polym. Phys. 37 (1999) 2463–2475.
[35] Z.P. Smith, G. Hernández, K.L. Gleason, A. Anand, C.M. Doherty, K. Konstas, C. Alvarez, A.J. Hill, A.E. Lozano, D.R. Paul, B.D. Freeman, Effect of polymer structure on gas transport properties of selected aromatic polyimides, polyamides and TR polymers, J. Membr. Sci. 493 (2015) 766–781.
[36] G.K. Fleming, W.J. Koros, Dilation of polymers by sorption of carbon dioxide at elevated pressures. 1. Silicone rubber and unconditioned polycarbonate, Macromolecules 19 (1986) 2285–2291.
[37] P. Li, T.S. Chung, D.R. Paul, Gas sorption and permeation in PIM-1, J. Membr. Sci. 432 (2013) 50–57.
[38] P. Li, T.S. Chung, D.R. Paul, Temperature dependence of gas sorption and permeation in PIM-1, J. Membr. Sci. 450 (2014) 380–388.
[39] T.T. Moore, W.J. Koros, Gas sorption in polymers, molecular sieves, and mixed matrix membranes, J. Appl. Polym. Sci. 104 (2007) 4053–4059.
[40] B.J. Story, W.J. Koros, Sorption and transport of CO_2 and CH_4 in chemically modified poly(phenylene oxide), J. Membr. Sci. 67 (1992) 191–210.
[41] V.I. Bondar, Y. Kamiya, Y. Yampolskii, On pressure dependence of the parameters of the dual-mode sorption model, J. Polym. Sci. B: Polym. Phys. 34 (1996) 369–378.
[42] K.A. Stevens, Z.P. Smith, K.L. Gleason, M. Galizia, D.R. Paul, B.D. Freeman, Influence of temperature on gas solubility in thermally rearranged (TR) polymers, J. Membr. Sci. 533 (2017) 75–83.
[43] W.J. Koros, D.R. Paul, CO_2 sorption in poly(ethylene terephthalate) above and below the glass transition, J. Polym. Sci.: Polym. Phys. Ed. 16 (1978) 1947–1963.
[44] T.C. Merkel, V.I. Bondar, K. Nagai, B.D. Freeman, Sorption and transport of hydrocarbon and perfluorocarbon gases in poly(1-trimethylsilyl-1-propyne), J. Polym. Sci. B: Polym. Phys. 38 (2000) 273–296.
[45] R.H. Perry, D.W. Green, Chemical Engineers' Handbook, 7th ed., McGraw-Hill, 1999.
[46] J. Ran, M.W. Wong, Saturated hydrocarbon-benzene complexes: theoretical study of cooperative CH/π interactions, J. Phys. Chem. A 119 (2006) 9702–9709.
[47] B.J. Story, W.J. Koros, Sorption of CO_2/CH_4 mixtures in poly(phenylene oxide) and a carboxylated derivatives, J. Appl. Polym. Sci. 42 (1991) 2613–2626.
[48] R.D. Raharjo, B.D. Freeman, E.S. Sanders, Pure and mixed gas CH_4 and n-C_4H_{10} sorption and dilation in poly(1-trimethylsilyl-1-propyne), Polymer 48 (2007) 6097–6114.
[49] O. Vopicka, De Angelis, Sarti, Mixed gas sorption in glassy polymeric membranes: i. CO_2/CH_4 and n-C_4/CH_4 mixtures sorption in poly(1-trimethylsilyl-1-propyne) (PTMSP), J. Membr. Sci. 449 (2014) 97–108.
[50] A.E. Gemeda, M.G. De Angelis, N. Du, N. Li, M.D. Guiver, G.C. Sarti, Mixed gas sorption in glassy polymeric membranes. III. CO_2/CH_4 mixtures in a polymer of intrinsic microporosity (PIM-1): effect of temperature, J. Membr. Sci. 524 (2017) 746–757.
[51] A.C. Puleo, D.R. Paul, S.S. Kelley, The effect of degree of acetylation on gas sorption and transport behavior in cellulose acetate, J. Membr. Sci. 47 (1989) 301–332.
[52] A.J. Erb, D.R. Paul, Gas sorption and gtransport in polysulfone, J. Membr. Sci. 8 (1981) 11–22.
[53] P. Meares, The diffusion of water through polyvinyl acetate, J. Am. Chem. Soc. 76 (1954) 3415–3422.
[54] C.A. Scholes, B.D. Freeman, S.E. Kentish, Water vapor permeability and competitive sorption in thermally rearranged (TR) membranes, J. Membr. Sci. 470 (2014) 132–137.
[55] B. Comesana-Gandara, L. Ansaloni, Y.M. Lee, A.E. Lozano, M.G. De Angelis, Sorption, diffusion, and permeability of humid gases and aging of thermally rearranged (TR) polymer membranes from a novel ortho-hydroxypolyimide, J. Membr. Sci. 542 (2017) 439–455.
[56] K.A. Lokhandwala, S.M. Nadakatti, S.A. Stern, Solubility and transport of water vapor in some 6FDA-based polyimides, J. Polym. Sci. B: Polym. Phys. 33 (1995) 965–975.
[57] O. Vopicka, K. Friess, V. Hynek, P. Sysel, M. Zgazar, M. Sipek, K. Pilnacek, M. Lanc, J.C. Jansen, C.R. Mason, P.M. Budd, Equilibrium and transient sorption of vapours and gases in the polymer of intrinsic microporosity PIM-1, J. Membr. Sci. 434 (2013) 148–160.
[58] J. Crank, The Mathematics of Diffusion, 2nd ed., Oxford University Press, Oxford, 1975.
[59] S.K. Burgess, D.S. Mikkilineni, D.B. Yu, D.J. Kim, C.R. Mubarak, R.M. Kriegel, W.J. Koros, Water sorption in poly(ethylene furanoate) compared to poly(ethylene terephthalate). Part 1: equilibrium sorption, Polymer 55 (2014) 6861–6869.
[60] P. Musto, M. Galizia, M. Pannico, G. Scherillo, G. Mensitieri, Time-resolved Fourier transform infrared spectroscopy, gravimetry, and thermodynamic modeling for a molecular level description of water sorption in Poly(ε-caprolactone), J. Phys. Chem. B 118 (2014) 7414–7429.
[61] G. Scherillo, M. Galizia, P. Musto, G. Mensitieri, Water sorption thermodynamics in glassy and rubbery polymers: modeling the interactional issues emerging from FTIR spectroscopy, Ind. Eng. Chem. Res. 52 (2013) 8674–8691.
[62] F. Doghieri, G.C. Sarti, Solubility, diffusivity, and mobility of n-pentane and ethanol in poly(1-trimethylsilyl-1-propyne), J. Polym. Sci. B: Polym. Phys. 35 (1997) 2245–2258.